Transportation Research Part B 81 (2015) 520–538

Contents lists available at ScienceDirect

Transportation Research Part B

journal homepage: www.elsevier.com/locate/trb

Urban transportation emissions mitigation: Coupling high-resolution vehicular emissions and traffic models for traffic signal optimization

Carolina Osorio *, Kanchana Nanduri

Department of Civil & Environmental Engineering, Massachusetts Institute of Technology, Cambridge, MA 02139, USA

ARTICLE INFO

Article history:
Received 18 June 2014
Received in revised form 11 December 2014
Accepted 29 December 2014
Available online 4 May 2015

Keywords:
Microscopic simulation
Simulation-based optimization
Urban vehicular emissions
Signal control

ABSTRACT

This paper proposes a methodology that allows high-resolution traffic and emissions models, known as microscopic simulation models, to be efficiently used to address transportation optimization problems that account for complex environmental metrics. The methodology consists of a metamodel simulation-based optimization (SO) approach. The metamodel combines traffic and emissions information from high-resolution microscopic simulators with information from lower-resolution analytical macroscopic models. This paper formulates and uses an analytical and differentiable macroscopic approximation of the non-differentiable simulation-based microscopic emissions model. A differentiable macroscopic traffic model is also used.

This paper shows that the analytical structural information provided by macroscopic analytical emissions models can contribute, despite their lower-resolution, to enhance the computational efficiency of algorithms that embed higher-resolution inefficient emissions models. The proposed algorithm is computationally efficient, i.e., it can identify points with improved performance within few simulation runs. More generally, the results of this paper highlight the added value of embedding analytical structural information within SO algorithms to address complex SO problems.

A traffic signal control case study is carried out. The proposed metamodel identifies signal plans that improve travel time and various emissions metrics. We present the corresponding monetary savings that can be achieved.

This optimization framework enables practitioners to use high-resolution microscopic traffic and emissions models to systematically design transportation schemes that account directly, in the design process, for environmental metrics. Hence, the use of such high-resolution models is no longer limited to the environmental evaluation of a small set of predetermined schemes. The tight computational budgets used in this paper show that such complex problems can be addressed in a computationally efficient manner.

1. Introduction

Nations around the world have adopted increasingly stringent regulations to monitor and control urban traffic emissions. In the US, federal regulations such as the Clean Air Act and the Surface Transportation Efficiency Act place increasing

* Corresponding author. Tel.: +1 617 452 3063.
E-mail address: osorioc@mit.edu (C. Osorio).

http://dx.doi.org/10.1016/j.trb.2014.12.007
0191-2615/

responsibility on transportation agencies to account for and achieve their environmental targets. By increasing accountability and using past performance as a metric for the procurement of future federal funding, these regulations also build incentive for agencies to design and operate their networks in a more sustainable manner.

Transportation agencies currently design transportation schemes (e.g., network design, traffic management) with a focus on improving traditional traffic metrics (e.g., travel times, throughput), they then evaluate the environmental impact of a small set of pre-determined schemes. There is a lack of practical, computationally efficient, optimization techniques that enable them to design the schemes while directly accounting for complex environmental metrics. This paper addresses this challenge.

The efficient design of such schemes involves coupling urban traffic models with vehicle emissions models, and embedding the integrated models within efficient optimization algorithms. Traffic models are usually classified as either macroscopic, mesoscopic or microscopic. For a recent review, see Barceló (2010). Macroscopic models are aggregate, flow-based models that are often computationally tractable and scalable yet fail to account for vehicle-specific attributes or detailed traffic dynamics. Microscopic models represent individual vehicles and individual travelers, they can account for the heterogeneity of driver, and more generally traveler, behavior; yet are often stochastic and computationally costly to run, this makes their efficient use for transportation optimization a challenge. Mesoscopic models combine ideas from both macroscopic and microscopic models.

Similarly, emissions models can be classified as either macroscopic or microscopic. For reviews see Rakha et al. (2003), Cappiello (2002), and Williams et al. (2001). Macroscopic emissions models are usually based on laboratory drive cycle tests conducted over a given average speed (CARB, 2008; EPA, 1994). Once the emissions rates are established for a given average speed, the emissions at other speeds are estimated by using multiplicative speed correction factors (SCFs). SCFs are based on inputs of vehicle-specific characteristics such as age and operating conditions. Macroscopic models do not account for time-variations in speed, let alone in acceleration, which significantly impact emissions (Rakha et al., 2000).

Microscopic emissions models, on the other hand, are based on vehicle-specific instantaneous (e.g., second by second) speed and acceleration information. Other inputs include vehicle-specific information (e.g., type, age) and road information (e.g., road-grade). Microscopic emissions models provide a higher-resolution description of emissions compared to their macroscopic counterparts, yet are more data-intensive and hence their use is mostly limited to the analysis of small urban areas (e.g., a corridor segment).

This paper proposes an optimization framework that can address a variety of urban transportation problems while directly accounting for both instantaneous vehicular emissions metrics and traditional congestion metrics (e.g., travel times). The framework considers continuous generally constrained simulation-based optimization problems. A variety of sustainable urban traffic management problems can hence be addressed with this framework.

As is detailed in Section 1.1, there is extensive work that couples vehicular emissions and vehicular traffic models. Nonetheless, the majority of the work uses the coupled models to evaluate a small set of predetermined transportation strategies (e.g., traffic management strategies). This paper uses the coupled models for optimization. It proposes an optimization framework that allows transportation strategies with improved emissions performance to be systematically designed.

To illustrate the approach, we consider a traffic signal control problem. The mapping of signal plans to network-wide vehicular emissions depends in an intricate way on individual vehicle technologies, instantaneous driver behavior and prevailing local traffic conditions. Hence, it is a nonlinear and high-variance function with numerous local minima. This makes the use of instantaneous emissions metrics for network-wide optimization an intricate problem. The proposed optimization method addresses this problem: it embeds high-resolution instantaneous emissions models and identifies traffic signal plans that improve network-wide congestion and emissions metrics.

The proposed optimization framework is computationally efficient, i.e., strategies with improved performance can be identified within few simulation runs. This is of interest for practitioners. In order to achieve computational efficiency, this paper formulates a macroscopic analytical and differentiable emissions model that approximates the non-differentiable microscopic simulation-based emissions model. Information from both the macroscopic and the microscopic models is combined within a simulation-based optimization algorithm. This allows the algorithm to use both high-resolution information (from the microscopic model) and analytical computationally efficient information (from the macroscopic model). It is this combination that allows the inefficient microscopic simulator to be used efficiently for optimization.

Section 1.1 reviews work that has coupled vehicular traffic and emissions models to address various transportation problems. Section 1.2 details how this paper contributes to the simulation-based optimization literature.

1.1. Coupling of vehicular traffic and emissions models for transportation analysis

A summary of this review is given in Table 1. This table lists for each work the type of traffic and emissions model used, and whether the coupled models are used for the what-if analysis of a small set of predetermined transportation strategies or for optimization. The last line considers the method presented in this paper.

The works of Li et al. (2004) and of Williams et al. (2001) couple macroscopic traffic models and macroscopic emissions models of carbon monoxide (CO), hydrocarbons (HC) and nitrogen oxides (NO_x). They use the coupled models to evaluate the impact on delays, fuel consumption and emissions of various traffic signal plan parameters. Li et al. (2004) consider a case study of one intersection in the Chinese city of Nanjing. Williams et al. (2001) study hypothetical networks with up to two

Table 1
Vehicular traffic and emissions model used for either what-if analysis or optimization.

	Traffic model			Emissions model		What-if analysis	Optimization
	Micro.	Meso.	Macro.	Micro.	Macro.		
Li et al. (2004)			✓		✓	✓	
Williams et al. (2001)			✓		✓	✓	
Rakha et al. (2004)	✓			✓		✓	
Bai et al. (2007)		✓			✓	✓	
Bartin et al. (2007)	✓				✓	✓	
Xie et al. (2011)	✓				✓	✓	
Madireddy et al. (2011)	✓			✓		✓	
Liu and Tate (2000)	✓				✓	✓	
Panis et al. (2006)	✓			✓		✓	
Cappiello (2002)		✓		✓		✓	
Lin et al. (2011)		✓		✓		✓	
Lee et al. (2009)	✓			✓	✓	✓	
Ahn and Rakha (2008)	✓			✓		✓	
Zegeye et al. (2010)			✓	✓			✓
Zhang et al. (2013)			✓		✓		✓
Stevanovic et al. (2009)	✓			✓			✓
Osorio and Nanduri	✓		✓	✓	✓		✓

intersections. Rakha et al. (2000) couple a microscopic emissions model (VT-Micro; Rakha et al., 2004) with a microscopic traffic model (INTEGRATION; Van Aerde, 1999) to evaluate the performance of a set of predetermined traffic signal plans for a four-link network.

Bai et al. (2007) combine the mesoscopic traffic model DYNASMART-P (Mahmassani and Sbayti, 2004) with the macroscopic emissions model EMFAC (CARB, 2008) to study the effect of changes in regional demand on emissions. Bartin et al. (2007) analyze the emissions impacts of introducing electronic toll collection systems on the New Jersey Turnpike (New Jersey, USA) using a microscopic traffic model PARAMICS (Quadstone, 2009) in combination with the macroscopic emissions model MOBILE6.2 (EPA, 2003). Xie et al. (2011) study the effect of various vehicle fleet compositions (e.g., electric cars, biofuel cars) on pollutant emissions of CO, NO_x, sulfur oxides (SO_x) and carbon dioxide (CO_2). They study a highway segment in Greenville (South Carolina, USA). Xie et al. (2011) couple PARAMICS with the emissions model MOVES (EPA, 2010) which has the capability of estimating microscopic emissions. However, in the study MOVES is used in a macroscopic context by providing only link-level average speeds as inputs. PARAMICS is also combined with a microscopic emissions model (VERSIT+; Smit et al., 2007) by Madireddy et al. (2011), who evaluate the impact of various speed limit reductions on emissions of CO_2 and NO_x for an area in Antwerp, Belgium.

In Liu and Tate (2000), a what-if analysis is carried out to study the impact of intelligent speed adaptation systems on CO, HC and NO_x. A microscopic traffic model (DRACULA; Liu et al., 11:20) along with a macroscopic emissions model (QUARTET, 1992) are used. The impact of intelligent speed adaptation systems is also studied in Panis et al. (2006) with a microscopic emissions model of CO_2, NO_x, volatile organic compounds (VOC) and particulate matter (PM), along with a microscopic traffic model (DRACULA). They consider an area within the Belgian city of Ghent.

Cappiello (2002) integrate a microscopic emissions model (of CO_2, CO, HC and NO_x), with a mesoscopic traffic model. They use the combined model to evaluate the performance of various variable message sign strategies on a hypothetical 14-link network. Lin et al. (2011) couple a mesoscopic traffic simulator (DynusT; Chiu et al., 2011) with the microscopic emissions model MOVES in order to evaluate the impact on CO_2 emissions of various congestion management schemes in Sacramento (California, USA). Lee et al. (2009) use a microscopic traffic simulator (TransModeler; Caliper, 2008) in combination with both a microscopic emissions model (CMEM; Scora et al., 2006), which is used to estimate CO, CO_2, HC and NO_x, and a macroscopic emissions model (EMFAC; CARB, 2008), which is used to estimate PM. They study the impacts of heavy-duty truck traffic along a highway leading to a container port facility in Alameda (California, USA). Microscopic emissions (VT-Micro) and microscopic traffic (INTEGRATION) models are also used by Ahn and Rakha (2008) to evaluate the impact of route choice decisions on emissions. They also carry out a comparative analysis of the emissions estimates between macroscopic and microscopic models. They recommend the use of microscopic emissions models in order to account for the time-dependent vehicle-level variations of speeds and accelerations.

Several works have coupled traffic and emissions models for optimization. The most common approach has been the use of macroscopic traffic and macroscopic emissions models. For instance, Zegeye et al. (2010) integrate a macroscopic traffic model (METANET; Messmer and Papageorgiou, 1990) with a microscopic CO_2 emissions model (VT-Micro). In this work the average link speeds and accelerations provided by the macroscopic traffic model are used as inputs into the microscopic emissions model as if they were vehicle-specific instantaneous measures. The combined models are embedded within a dynamic control framework and used to address a dynamic speed limit problem for a hypothetical 12 km 2-lane freeway. Similarly, Zhang et al. (2013) consider a macroscopic traffic model along with a macroscopic emissions model, and address a bi-objective signal control problem that minimizes both delay and a pollutant exposure metric that accounts for the concentration of several roadside pollutants.

Microscopic simulators coupled with microscopic emissions models provide the highest-resolution approach since they account for: (i) detailed vehicle-to-vehicle and vehicle-to-supply interactions, (ii) instantaneous speed and acceleration information, (iii) vehicle-specific attributes (e.g., vehicle type, age). All these factors affect emissions, and should be accounted for in order to yield accurate emissions estimates. Hence, coupled microscopic traffic and microscopic emissions models is an appropriate tool to design transportation schemes that account for emissions (Bartin et al., 2007). However, due to the complexity and computational inefficiency of microscopic traffic and emissions models, their use is mostly limited to what-if analysis, i.e., to evaluate the performance of a pre-determined small set of transportation schemes, rather than to perform optimization.

To the best of our knowledge, the only work that has coupled microscopic traffic and microscopic emissions models for emissions optimization is that of Stevanovic et al. (2009). Stevanovic et al. (2009) integrate a microscopic traffic model (VISSIM; PTV, 2008) with a microscopic emissions model (CMEM; Scora et al., 2006). They embed the integrated models within a genetic algorithm tailored for traffic signal control problems (VISGAOST; Stevanovic et al., 2008). They study a network of 2 arterials with 14 signalized intersections in Park City (Utah, USA). Their objective function accounts for throughput, stops, delay, fuel consumption and CO_2 emissions. They consider a signal control problem with over 100 decision variables, and address it within a total of 60,000 simulation runs (12,000 signal plans are evaluated across 5 simulation replications each). Note that the work of Kwak et al. (2012) and of Park et al. (2009) use microscopic traffic and microscopic emissions models (TRANSIMS, CORSIM and VT-Micro) to optimize either total queueing time or fuel consumption, the effect on emissions is evaluated a posteriori. These works also use a genetic algorithm approach.

In the field of signal control, the most popular algorithm used when considering complex objective functions (such as emissions) or complex models (such as microscopic models) are genetic algorithms (GA). The use of GA allows for a variety of complex signal control problems to be addressed, yet these algorithms are not designed to address problems in an efficient manner, e.g., under tight computational budgets. GA case studies are typically designed such as to evaluate tens of thousands of points (Kwak et al., 2012; Stevanovic et al., 2009; Park et al., 2009). As Kwak et al. (2012) state in their closing remarks: "more efficient computational techniques should be sought and implemented. Although the GA worked well, it consumed much time and computational loads. Faster computational techniques would promise quicker adoption by practitioners".

In this paper, we propose a computationally efficient simulation-based optimization (SO) technique that uses integrated microscopic traffic and microscopic emissions models to design traffic signal control strategies that account for both traditional traffic metrics and emissions metrics. Signal control remains a low cost alternative to emissions mitigation. The framework presented in this paper enables practitioners to use state-of-the-art traffic and emissions models to go beyond evaluation purposes and instead systematically identify schemes that mitigate both congestion and emissions. Additionally, the focus of this paper is to propose an SO technique that while using complex inefficient simulators can address transportation problems in a computationally efficient manner. That is, the SO technique can identify schemes with improved performance within few simulation runs.

The proposed SO framework is able to identify signal plans with improved performance of various metrics and it is able to do so within a tight computational budget (e.g., in the case study of Section 4, we allow for a maximum 150 simulation runs, as opposed to tens of thousands of runs). We illustrate how the proposed method identifies signal plans with improved performance both at the network-level and the link-level, while resorting to disaggregate and high-variance vehicle-specific information.

1.2. Simulation-based optimization framework

We use the simulation-based optimization (SO) framework of Osorio and Bierlaire (2013), which considers continuous nonlinear generally constrained optimization problems, where the objective function is derived from a stochastic simulator, i.e. a closed-form expression is not available for the objective function, whereas closed-form analytical expressions are available for all constraints.

The problems considered are of the form:

$$\min_{x} \quad f(x,z;p) \tag{1}$$

$$g(x,z;p) = 0. \tag{2}$$

The feasible space is defined by g which is a set of general, typically nonconvex, analytical and differentiable constraints. Note that any type of analytical constraint (e.g., inequality, bound) can be formulated in the form of an equality as in (2). Hence, g represents a general set of constraints. The objective function f can be, for instance, the expected value of a given stochastic performance measure $F : f(x,z;p) = E[F(x,z;p)]$. The decision vector x is real-valued (e.g., green times), z denotes other endogenous variables (e.g., departure-time/mode/route choice probabilities), and p denotes the deterministic exogenous parameters (e.g., network topology).

This SO algorithm is a metamodel technique. At every iteration i, three main steps are carried out: (i) an analytical approximation of the objective function f is fitted based on the set of simulation observations collected so far, this approximation is known as a metamodel, (ii) the metamodel is then used to perform optimization and derive a trial point, (iii) the performance of the trial point is evaluated with the simulator, which leads to new simulation observations. As new

simulated observations become available, the accuracy of the metamodel can be improved, leading to trial points with further improved performance. These steps are iterated until, for instance, the computational budget is depleted.

The main idea underlying the SO framework of Osorio and Bierlaire (2013) is to consider a metamodel that combines information from the microscopic simulator with information from an analytical macroscopic model. The general functional form of the metamodel at a given iteration i is:

$$m_i(x, y; \alpha_i, \beta_i, q) = \alpha_i f_A(x, y; q) + \phi(x; \beta_i), \tag{3}$$

where ϕ denotes a general-purpose metamodel component (a polynomial quadratic in x with diagonal second-derivative matrix is used), f_A is known as the physical metamodel component and represents the approximation of the objective function (f of Eq. (1)) as derived by the macroscopic model. The metamodel may also depend on endogenous macroscopic model variables y (e.g., queue-length distributions), exogenous macroscopic parameters q (e.g., total demand), and a set of metamodel parameters α_i and β_i, which are iteratively fitted based on simulation observations.

The metamodel can be interpreted as an approximation of the objective function f provided by the macroscopic model, which is corrected parametrically by both a scaling factor (α) and a separable error term $\phi(x; \beta)$. The general-purpose metamodel component ensures asymptotic metamodel properties (necessary for convergence analysis) (Osorio and Bierlaire, 2013).

For a given problem as formulated in (1) and (2), the SO algorithm solves at iteration i a problem with the following form:

$$\min_x \quad m_i(x, y; \alpha_i, \beta_i, q) \tag{4}$$

$$g(x, z; p) = 0 \tag{5}$$

$$h(x, y; q) = 0. \tag{6}$$

Compared to Problem (1) and (2): the objective function has been approximated by the metamodel, and there are a new set of constraints (6), which represent the macroscopic model. The use of the macroscopic model: (i) allows for the functional form of the metamodel to be problem-specific (since the form of f_A is problem-specific), (ii) provides the SO problem (1) and (2) with analytical structural information. That is, the macroscopic model (Constraint (6)) provides analytical, tractable, and differentiable information about how the decision variables are related (in an intricate way) to the considered objective function. Together these two features allow the SO algorithm to identify trial points with improved performance within few simulation runs. That is, they enable inefficient microscopic simulators to be used efficiently to address various transportation optimization problems.

This general SO framework has been successfully used to address transportation optimization problems with traditional objective functions (e.g., expected travel time, expected flows) (Osorio and Chong, forthcoming; Osorio et al., 2014b,a), which can be accurately approximated with analytical macroscopic models. More recently, we have formulated the general framework to account for fuel consumption metrics (Osorio and Nanduri, forthcoming). Nonetheless, the potential of such an SO framework to address problems where the objective function depends on metrics that are not accurately approximated with macroscopic models is an open question.

This paper considers emissions metrics. As mentioned above, the latter depend on detailed information of: (i) vehicle-specific attributes (type, engine technology), (ii) driver behavior (e.g., vehicle-to-vehicle and vehicle-to-supply interactions), (iii) instantaneous, and complex, local speed and acceleration patterns. Since macroscopic analytical emissions models do not account for such details, they provide a lower-resolution description of emissions patterns. This paper investigates whether the analytical structural information of macroscopic emissions models can contribute, despite their lower-resolution, to enhance the computational efficiency of simulation-based optimization algorithms. The analysis of this paper emphasizes the added value, for general simulation-based optimization problems, of embedding analytical structural information (Constraint (6)), even when an accurate analytical approximation of the objective function is not available (inaccuracy of f_A in (3)).

Microscopic emissions models, such as the one used in this paper, are often non-differentiable. For the SO framework to be efficient an analytical and differentiable macroscopic approximation needs to be derived, i.e., f_A needs to be differentiable. This paper formulates a macroscopic analytical and differentiable approximation of the non-differentiable microscopic emissions model. The use of a differentiable model is key to designing a computationally efficient optimization framework.

2. Traffic signal control problem

A review of traffic signal control terminology and formulations are given in Appendix A of Osorio et al. (2010) and in Lin et al. (2011). In this paper, we consider a fixed-time (also called time of day or pre-timed) control strategy. These are strategies that use historical traffic patterns to derive a fixed signal plan for a given time period. The signal control problem is solved offline. The signal plans of multiple intersections are determined jointly. The decision variables are the green splits (i.e., green times) of the phases of the different intersections. All other traditional control variables (e.g., cycle times, offsets, stage structure) are assumed fixed.

We introduce the following notation:

b_i available cycle ratio of intersection i;
$x(j)$ green split of phase j;
x_L vector of minimal green splits;
$\mathcal{I}$ set of intersection indices;
$\mathcal{P}_I(i)$ set of phase indices of intersection$i$.

The problem is formulated as follows:

$$\min_x \quad f^{T,EM}(x;p) \tag{7}$$

$$\sum_{j\in\mathcal{P}_I(i)} x(j) = b_i, \quad \forall i \in \mathcal{I} \tag{8}$$

$$x \geqslant x_L, \tag{9}$$

where the decision vector x consists of the green splits for each phase. Constraints (8) ensure that for a given intersection the available cycle time is distributed among all phases. Green splits have lower bounds (Eq. (9)), which are set to 4 s in this work (following the Swiss transportation norms VSS (1992)).

The objective function is a linear combination of expected travel time f^T and the expected total emissions of four pollutants namely carbon dioxide, nitrogen oxides, volatile organic compounds and particulate matter, denoted as $f^{CO_2}, f^{NO_x}, f^{VOC}$ and f^{PM} respectively, and given by:

$$f^{T,EM} = \frac{w^T}{n^T} f^T + \frac{w^{CO_2}}{n^{CO_2}} f^{CO_2} + \frac{w^{NO_x}}{n^{NO_x}} f^{NO_x} + \frac{w^{VOC}}{n^{VOC}} f^{VOC} + \frac{w^{PM}}{n^{PM}} f^{PM}, \tag{10}$$

where $w^T, w^{CO_2}, w^{NO_x}, w^{VOC}$ and w^{PM} are economic weighting parameters for travel time and the pollutants CO_2, NO_x, VOC and PM, respectively. While w^T denotes the value of time, the weights for each of the pollutants are based on their externality costs to human health and other large-scale effects such as global warming. The values of the weighting parameters are derived from Table 2 and Table 9 of Mayeres et al. (1996), and listed in Table 5 of Appendix A of this paper. The parameters $n^T, n^{CO_2}, n^{NO_x}, n^{VOC}$ and n^{PM} are normalization constants. The use of such constants follows the formulation in Li et al. (2004). The values of the normalization constants are estimates for $f^T, f^{CO_2}, f^{NO_x}, f^{VOC}$ and f^{PM}, obtained from a benchmark signal plan. In Section 4, we consider an area within the Swiss city of Lausanne. The normalization constants are given by the performance estimates (of travel time, CO_2, NO_x, etc.) obtained under an existing fixed-time signal plan for the city of Lausanne. Their numerical values are given in Table 5 of Appendix A.

3. Models

This section presents the microscopic and macroscopic traffic models (Section 3.1), and the microscopic and macroscopic emissions models (Section 3.2). Section 3.4 summarizes the proposed methodology.

3.1. Traffic models

We use the same traffic models as in Osorio and Bierlaire (2013).

Microscopic simulation model. The calibrated microscopic model of the Swiss city of Lausanne (Dumont and Bert, 2006) is used. Evening peak period traffic (5–6 pm) is considered. This model represents individual vehicles in the network, it simulates an average demand of approximately 12,400 trips over the entire city. Trips are generated based on an origin–destination matrix, along with a stochastic headway model. The simulation model accounts for the heterogeneous behavior of individual drivers by using car following, lane changing, gap acceptance and route choice models. It is implemented with the Aimsun traffic simulation software (TSS, 2011).

Macroscopic analytical model. We use an analytical queueing network model formulated in Osorio et al. (2010, Chapter 4) and Osorio and Bierlaire (2009). Each lane of a road is modeled as one (or a set of) finite capacity Markovian queue(s). The spatial propagation of congestion is modeled through the queueing-theoretic notion of blocking. The analytical traffic model combines ideas from finite capacity queueing network theory, national transportation norms, and other urban traffic models. It is formulated as a system of nonlinear equations. Its formulation is given in Appendix A.

3.2. Emissions models

3.2.1. Microscopic model

We use the microscopic emissions model embedded in Aimsun (v6.1), which is based on the model of Panis et al., 2006. This model gives the instantaneous emissions rate of four pollutants namely CO_2, NO_x, VOC and PM, based on a vehicle's instantaneous speed and acceleration. We introduce the following notation for a given vehicle j:

k	Pollutant type, $k \in \{CO_2, NO_x, VOC, PM\}$;
$v_j(t)$	Instantaneous speed (inm/s);
$a_j(t)$	Instantaneous acceleration (inm/s^2);
$ER_j^k(t)$	Instantaneous emissions rate of pollutant k(ing/s);
E_{0j}^k	Minimum emissions rate of pollutant k(ing/s);
$C_{1j}^k, C_{2j}^k, C_{3j}^k, C_{4j}^k, C_{5j}^k, C_{6j}^k$	Emissions rate coefficients for pollutant k.

The emissions rate for vehicle j at a given time-instant t is given by (cf. Eq. (4) in Panis et al. (2006)):

$$ER_j^k(t) = \max\left\{E_{0j}^k; C_{1j}^k + C_{2j}^k v_j(t) + C_{3j}^k v_j(t)^2 + C_{4j}^k a_j(t) + C_{5j}^k a_j(t)^2 + C_{6j}^k v_j(t) a_j(t)\right\}. \tag{11}$$

Eq. (11) holds for CO_2 or PM emissions. For NO_x and VOC emissions, the emissions rate coefficients differ depending on whether the vehicle is in acceleration or deceleration mode. If $a_j(t) \geqslant -0.5$ m/s, then

$$ER_j^k(t) = \max\left\{E_{0j}^k; C_{1j}^k + C_{2j}^k v_j(t) + C_{3j}^k v_j(t)^2 + C_{4(1)j}^k a_j(t) + C_{5(1)j}^k a_j(t)^2 + C_{6(1)j}^k v_j(t) a_j(t)\right\}. \tag{12}$$

Otherwise, if $a_j(t) < -0.5$ m/s, then

$$ER_j^k(t) = \max\left\{E_{0j}^k; C_{1j}^k + C_{2j}^k v_j(t) + C_{3j}^k v_j(t)^2 + C_{4(2)j}^k a_j(t) + C_{5(2)j}^k a_j(t)^2 + C_{6(2)j}^k v_j(t) a_j(t)\right\}. \tag{13}$$

In Panis et al. (2006), the minimum emissions rate E_{0j}^k is fixed to zero for all pollutant types and vehicle types. The emissions rate coefficients (e.g., C_{1j}^k, C_{2j}^k, etc.) are specified for each pollutant type and vehicle type, and were determined from emissions measurements of on-road instrumented vehicles (Panis et al., 2006).

Hereafter, we consider a single vehicle type (referred to as petrol car in Panis et al. (2006)). All vehicles in the simulation are of this model. This assumption can be easily relaxed. The values of the corresponding emissions rate parameters are listed in Table 5 of Appendix A.

3.2.2. Macroscopic model

As described in Section 3.1, the macroscopic traffic model represents an urban network as a finite capacity queueing network, where each road lane is represented by one (or possibly multiple) queues. Hereafter, we use the terms queue, lane and link interchangeably.

Recall that the purpose of the macroscopic emissions model is to provide a differentiable, analytical and tractable approximation of the microscopic emissions model (Eqs. (1)–(3)). This section describes how each emissions component of the objective function is approximated. In other words, we describe how the terms $f^{CO_2}, f^{NO_x}, f^{VOC}$ and f^{PM} of Eq. (10) are approximated.

For pollutant type k (where $k \in \{CO_2, NO_x, VOC, PM\}$), the expected total emissions (in g) in the network during the simulation period is approximated by:

$$E[TE^k] = \sum_{\ell \in \mathcal{L}} E\left[TE_\ell^k\right], \tag{14}$$

where $\mathcal{L}$ is the set of all links in the network, and $E[TE_\ell^k]$ denotes the expected total emissions (in g) of pollutant k on link ℓ. The latter is approximated by:

$$E[TE_\ell^k] = E[ER^{k,\ell}]E[T_\ell]\lambda_\ell \Delta T, \tag{15}$$

where $E[ER^{k,\ell}]$ denotes the expected emissions rate (in g/s) for link ℓ and pollutant type k, $E[T_\ell]$ is the expected travel time on link ℓ, λ_ℓ is the arrival rate to link ℓ and ΔT is the total simulation time. For a given link ℓ and pollutant type k, the term $\lambda_\ell \Delta T$ approximates the expected total demand over the time period of interest, while $E[ER^{k,\ell}]E[T_\ell]$ approximates the expected emissions per vehicle.

The expected emissions rate per link and pollutant type is approximated by using a simplified version of the Panis et al. (2006) model as given by:

$$E[ER^{k,\ell}] = \max\left\{E_0^k, C_1^k + C_2^k E[V_\ell] + C_3^k E[V_\ell]^2\right\}, \tag{16}$$

where E_0, C_1^k, C_2^k and C_3^k are vehicle parameters, and $E[V_\ell]$ is the expected vehicle speed on link ℓ. Eq. (16) is derived by making the following two simplifications to the microscopic emissions model (Eqs. (11)–(13)). First, we assume that throughout its trip in the considered network, a vehicle is in cruising mode. Thus, we substitute $a_j(t) = 0$ in Eqs. (11)–(13). Second, we assume that the emissions rate over a link ℓ for a vehicle in cruising mode is a function of average vehicle speed over that link (instead of instantaneous speed), i.e., we substitute $v_j(t)$ with $E[V_\ell]$. If different vehicle types are to be used, similar macroscopic emissions approximations can be derived for each vehicle type.

The above two simplifications are strong simplifications that are commonly used in macroscopic models, yet may lead to inaccurate emissions estimates. These simplifications contribute to the computational tractability of the macroscopic model. Additionally, recall that in this paper, the macroscopic model is not used as a stand-alone emissions model. Rather its emissions estimates are coupled with (more accurate) microscopic simulation-based emissions estimates (see Eq. (3)). This combination leads to a metamodel that can yield accurate emissions estimates, and can do so in a computationally tractable way.

The expected total emissions, across all pollutant types and all links, is given by:

$$E[TE] = \sum_{k\in\mathcal{K}} \frac{w^k}{n^k} E[TE^k] \tag{17}$$

where $\mathcal{K}$ denotes the set of pollutant types: $\mathcal{K} = \{CO_2, NO_x, VOC, PM\}$. We can substitute Eqs. (14) and (15) into (17) to obtain:

$$E[TE] = \sum_{k\in\mathcal{K}} \frac{w^k}{n^k} \sum_{\ell\in\mathcal{L}} E[TE_\ell^k] = \sum_{\ell\in\mathcal{L}} E[T_\ell]\lambda_\ell \Delta T \left(\sum_{k\in\mathcal{K}} \frac{w^k}{n^k} E[ER^{k,\ell}] \right). \tag{18}$$

The term $E[ER^{k,\ell}]$ is defined by Eq. (16), which is non-differentiable. The non-differentiable maximum operator of Eq. (16) ensures that the emissions rate of pollutant k on link ℓ is always non-negative since the minimum emissions rate E_0^k is set to zero for all pollutants and vehicle types (according to Table 2 of Panis et al. (2006)). A differentiable formulation is derived as follows.

We define two new variables for each link ℓ, $t_{1\ell}$ and $t_{2\ell}$, which are related to the analytical approximation of the expected emissions rates on link ℓ in the following way:

$$t_{1\ell} - t_{2\ell} = \sum_{k\in\mathcal{K}} \frac{w^k}{n^k} \left(C_1^k + C_2^k E[V_\ell] + C_3^k E[V_\ell]^2 \right). \tag{19}$$

Additionally, we impose lower bounds (equal to zero) for $t_{1\ell}$ and $t_{2\ell}$. Eq. (19) ensures that if the expected total emissions rate for a given link is positive, then it is equal to $t_{1\ell}$, and $t_{2\ell}$ equals zero. If the expected total emissions rate for the link is negative, then it is equal to the opposite of $t_{2\ell}$, and $t_{1\ell}$ equals zero. This implementation does not ensure that the expected emissions rate of each pollutant type k (where $k \in \{CO_2, NO_x, VOC, PM\}$) on link ℓ is non-negative. However, it does ensure that the expected total emissions rate on link ℓ is non-negative.

Since only non-negative emissions should appear in the objective function, the new analytical approximation to the expected total emissions (in g) in the network during the simulation is given by:

$$E[TE] = \sum_{\ell\in\mathcal{L}} E[T_\ell]\lambda_\ell \Delta T t_{1\ell}. \tag{20}$$

In order to analytically approximate the expected link travel time $E[T_\ell]$ and the expected link speed $E[V_\ell]$, the differentiable expressions of Osorio and Nanduri (forthcoming) are used. The expected link travel time is given by:

$$E[T_\ell] = \frac{E[N_\ell]}{\lambda_\ell (1 - P(N_\ell = s_\ell))}, \tag{21}$$

$$E[N_\ell] = \rho_\ell \left(\frac{1}{1-\rho_\ell} - \frac{(s_\ell + 1)\rho_\ell^{s_\ell}}{1 - \rho_\ell^{s_\ell+1}} \right), \tag{22}$$

where $E[N_\ell]$ is the expected number of vehicles on link ℓ, λ_ℓ is the arrival rate, s_ℓ is the queue's space capacity (i.e., upper bound on queue length), $P(N_\ell = s_\ell)$ is the probability that the queue is full (i.e., traffic spillback probability) and ρ_ℓ is known as the traffic intensity. The variables $\lambda_\ell, P(N_\ell = s_\ell)$ and ρ_ℓ are endogenous variables of the macroscopic traffic model and s_ℓ is an exogenous parameter (cf. Appendix A).

The expected link speed is given by:

$$E[V_\ell] = \lambda_\ell (1 - P(N_\ell = s_\ell)) \mathsf{L}_\ell / E[N_\ell], \tag{23}$$

where L_ℓ is an exogenous parameter that denotes the length of link ℓ.

In summary, an analytical and differentiable approximation of the expected total emissions over all pollutant types and all links is given by Eq. (20), which can be numerically evaluated by solving the System of Eqs. (19), (21)–(23) and (26).

3.3. Expected trip travel time metrics

The objective function (Eq. (10)) also contains the term f^T that represents the expected trip travel time. The microscopic simulator estimates this expectation by averaging the travel times of all completed trips during the simulation period. The macroscopic model uses the following analytical approximation of f^T:

$$E[T] = \frac{\sum_{\ell \in \mathcal{L}} E[N_\ell]}{\sum_{\ell \in \mathcal{L}} \gamma_\ell (1 - P(N_\ell = s_\ell))}, \tag{24}$$

where $E[T]$ represents the (macroscopic) expected trip travel time and γ_ℓ represents the external arrival rate to link ℓ (i.e., external demand). Eq. (24) is a direct application of Little's law (Little, 1961; Little, 2011) as applied to finite capacity networks (for more details, see Tijms, 2003, pp. 52–53).

3.4. Methodology summary

To summarize, the proposed methodology proceeds as follows. The metamodel SO algorithm of Osorio and Bierlaire (2013) is used. The metamodel is an analytical model that approximates the simulation-based objective function ($f^{T,EM}$ of Eq. (7)). The metamodel is defined by Eq. (3). It embeds an analytical approximation of the simulation-based objective function $f^{T,EM}$ provided by the macroscopic model. This analytical approximation is denoted by f_A in Eq. (3). At every iteration of the SO algorithm, the sample of microscopic simulation observations collected so far are used to fit the parameters of the metamodel, which are denoted α and β in Eq. (3). Hence, at every iteration of the SO algorithm the metamodel combines information from the analytical macroscopic model and the simulation-based microscopic model.

At iteration i, the metamodel m_i is used to solve the subproblem defined by Eqs. (4)–(6). Constraints (5) represent the signal control constraints, which are given by Eqs. (8) and (9). Constraints (6) represent the macroscopic traffic and emissions models, which are given by Eqs. (19)–(24) and (26). The macroscopic term of the metmodel (f_A of Eq. (3)) is given by:

$$f_A = \frac{w^T}{n^T} E[T] + E[TE], \tag{25}$$

where $E[T]$ is given by Eq. (24) and $E[TE]$ is given by Eq. (20).

For a signal control problem with n_1 endogenous signal phases that control a set of n_2 signalized queues within a network of a total of n_3 queues, the corresponding subproblem is implemented as a set of $n_1 + n_2 + 7n_3$ endogenous variables. The factor 7 corresponds to the traffic model (System (26)) being implemented as a set of 5 endogenous variables per queue and to the use of 2 emissions variables per queue $\ell : t_{1\ell}$ and $t_{2\ell}$ defined by Eq. (19).

4. Case study

4.1. Experimental setup

We use a model of the city of Lausanne that represents evening peak period traffic (Dumont and Bert, 2006). We consider the first hour of the evening peak period (5–6 pm). The network under consideration is located in the city center and is delimited by a circle in Fig. 1, the detailed network is displayed in the right plot of the figure. This network contains 47 roads and 15 intersections of which 9 are signalized. The signalized intersections have a cycle time of either 90 or 100 s and a total of 51 variable phases. This is a complex constrained simulation-based optimization problem.

The analytical queueing model of the network consists of 102 queues. The SO algorithm used in Osorio and Bierlaire (2013) is a derivative-free trust region algorithm. The trust region subproblem solved at each iteration consists of 825 variables with their corresponding lower bound constraints, 510 nonlinear equality constraints, 171 linear equality constraints and one nonlinear inequality constraint.

We compare the performance of the following three optimization methods.

- The proposed approach, denoted *Am*.

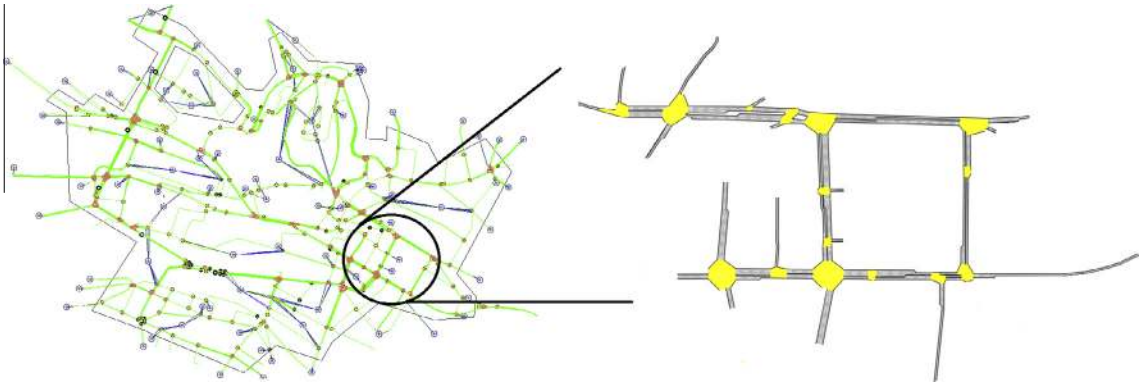

Fig. 1. Lausanne city network model (left), network of interest (right).

Table 2
Traffic and emissions models used by the compared methods.

	Traffic model		Emissions model	
	Microscopic (simulation-based)	Macroscopic (analytical)	Microscopic (simulation-based)	Macroscopic (analytical)
Am	✓	✓	✓	✓
$A\phi$	✓		✓	
Af_A		✓		✓

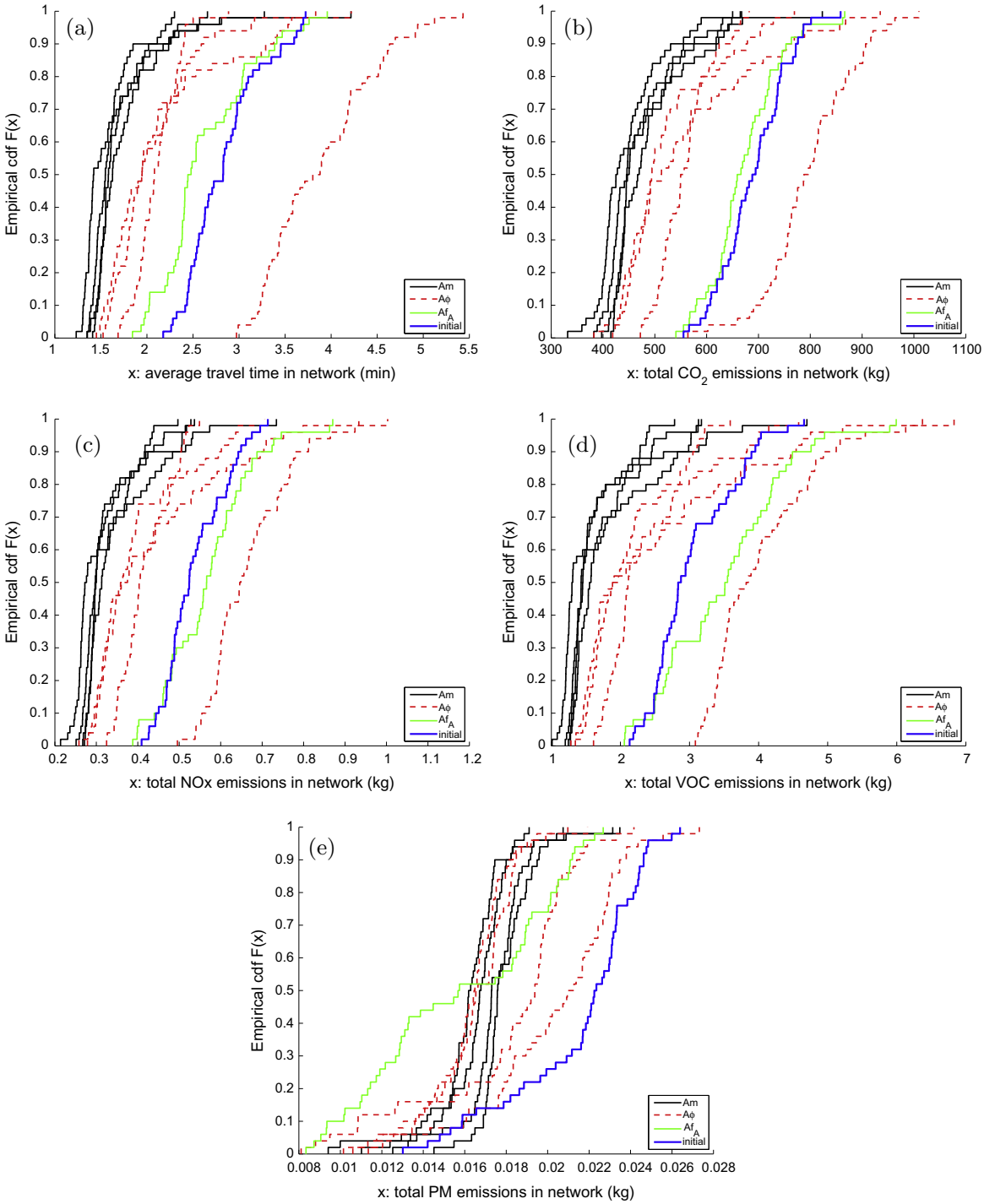

Fig. 2. Performance of the signal plans derived considering a random initial signal plan.

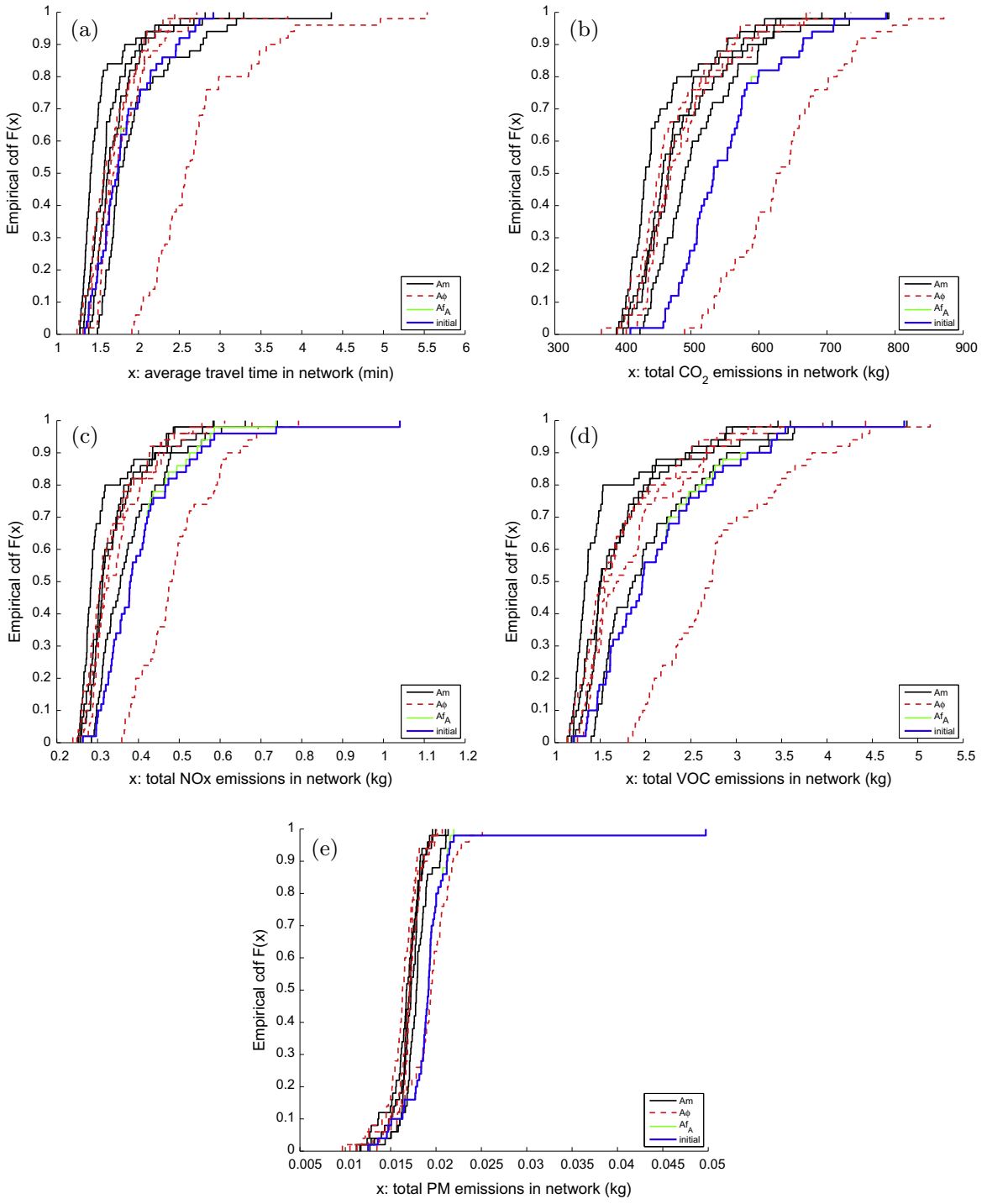

Fig. 3. Performance of the signal plans derived considering an existing signal plan for Lausanne as the initial plan.

- A traditional SO metamodel method, where the metamodel consists only of a quadratic polynomial with diagonal second derivative matrix (i.e., the metamodel consists of ϕ given in Eq. (3)). This approach therefore uses microscopic simulation information but does not use information from the macroscopic analytical traffic model. This approach is denoted $A\phi$. Note that for approach $A\phi$, the problem solved at every iteration of the SO algorithm is defined by Eqs. (4) and (5). Eq. (6), which represents the analytical traffic model, is not present.
- A method that uses only the analytical traffic model, and does not use any microscopic simulated information (i.e., the objective function is given by f_A in Eq. (3)). This method is denoted Af_A.

The types of traffic and emissions model used by each method are summarized in Table 2.

We consider different types of initial points: an existing fixed-time signal plan for Lausanne city (for details see Dumont and Bert, 2006), and randomly drawn feasible signal plans. The latter are uniformly drawn from the feasible region defined by Eqs. (8) and (9). We draw uniformly from this space using the code of Stafford (2006).

For methods *Am* and $A\phi$, we define the computational budget as a maximum of 150 simulation runs that can be carried out. That is, the algorithm starts off with no simulated information, and once it has called the simulator 150 times it stops. The point considered as the current iterate, which by definition is the best point identified so far, is then taken as the proposed signal plan. This is a very tight computational budget given the dimension and complexity of the considered problem.

For methods *Am* and $A\phi$, the derivation of a proposed signal plan involves calling the simulator. Given the stochastic nature of the simulation outputs, for a given initial point, the methods *Am* and $A\phi$ are run 4 times (allowing each time for a maximum of 150 simulation runs). In other words, each method (or algorithm) is launched 4 times. Each time a maximum of 150 simulation runs is allowed. We then compare the performance of all 4 proposed signal plans.

We evaluate the performance of a proposed signal plan as follows. We embed the proposed signal plan within the Lausanne microscopic simulation model. We then run 50 simulation replications, which yield 50 observations of the five performance measures of interest, namely expected travel time in the network and expected total emissions of CO_2, NO_x, VOC and PM in the network. For a given performance measure, we plot the cumulative distribution function (cdf) of these 50 observations.

4.2. Results

We compare the performance of the signal plans derived by each method in terms of the five different performance measures. Figs. 2 and 3 each contain five plots, one for each performance measure. Each plot displays 10 cdf curves. There are four solid black (resp. dashed red) curves, one for each of the signal plans proposed by the *Am* (resp. $A\phi$) method. The solid green cdf is for the signal plan proposed by Af_A, and the solid blue is for the initial signal plan.

Each cdf plot displays along the *x*-axis the considered performance measure. For a given *x* value, the *y*-axis displays the proportion of simulation replications (out of the 50 replications) that have a performance measure smaller than *x*. Hence, the more the cdf curves are shifted to the left, the higher the proportion of simulation replications with small performance measure values.

The main insights from these plots follow.

- All plans proposed by *Am* yield, for all five performance metrics, a systematic improvement compared to the initial plan. This is not the case for the plans of $A\phi$ or Af_A. In particular, one of the signal plans proposed by $A\phi$ does worse than the initial plan for four of the five metrics.
- For all metrics except PM (Plots 2(a)–(d)) the plans proposed by *Am* outperform all other plans.
- For the PM metric, the plans proposed by *Am* have: (i) similar or better performance than those proposed by $A\phi$, (ii) similar average performance but significantly lower variability than the plan of Af_A.
- The signal plan proposed by Af_A has mixed performance depending on the performance metric of interest.

In order to test whether the observed differences in performance are statistically significant, we perform a one-sided paired *t*-test. The *t*-statistics are displayed in Table 3. Each column considers one of the four signal plans proposed by *Am*,

Table 3
T-statistics considering a random initial signal plan.

	Am(1)	*Am*(2)	*Am*(3)	*Am*(4)
$A\phi(1)$	−20.09	−24.08	−19.37	−23.84
$A\phi(2)$	−6.95	−9.07	−6.12	−7.85
$A\phi(3)$	−3.70	−4.71	−5.61	−4.28
$A\phi(4)$	−2.04	−3.54	−2.84	−3.21
Af_A	−12.95	−15.18	−12.26	−14.48
Initial	−19.81	−18.78	−16.80	−25.79

Table 4
T-statistics considering an existing signal plan for Lausanne as the initial signal plan.

	Am(1)	*Am*(2)	*Am*(3)	*Am*(4)
$A\phi(1)$	**−13.17**	**−11.35**	**−12.09**	**−8.58**
$A\phi(2)$	−1.33	1.26	0.57	2.86
$A\phi(3)$	−1.47	1.22	0.32	3.11
$A\phi(4)$	**−2.38**	0.19	−0.48	1.88
Af_A	**−7.70**	**−5.52**	**−6.94**	**−2.96**
Initial	**−5.57**	**−3.89**	**−4.61**	**−2.58**

these signal plans are denoted $Am(1), Am(2), Am(3)$ and $Am(4)$. Each of the first four rows considers one of the four signal plans proposed by $A\phi$, these signal plans are denoted $A\phi(1), A\phi(2), A\phi(3)$ and $A\phi(4)$. The fifth row considers the signal plan proposed by Af_A, and the sixth row considers the initial signal plan. The statistic in column j and row i considers a t-test where the null hypothesis states that the expected value of the objective function of signal plans j and i are equal. The alternative hypothesis states that the expectation of signal plan j is lower than that of signal plan i. Each t-test considers a 5% significance level, and has 49 degrees of freedom. The critical value is -1.68. The table displays the corresponding t-statistics. All statistics are below the critical value and hence for all cases the null hypothesis is rejected, i.e., all signal plans proposed

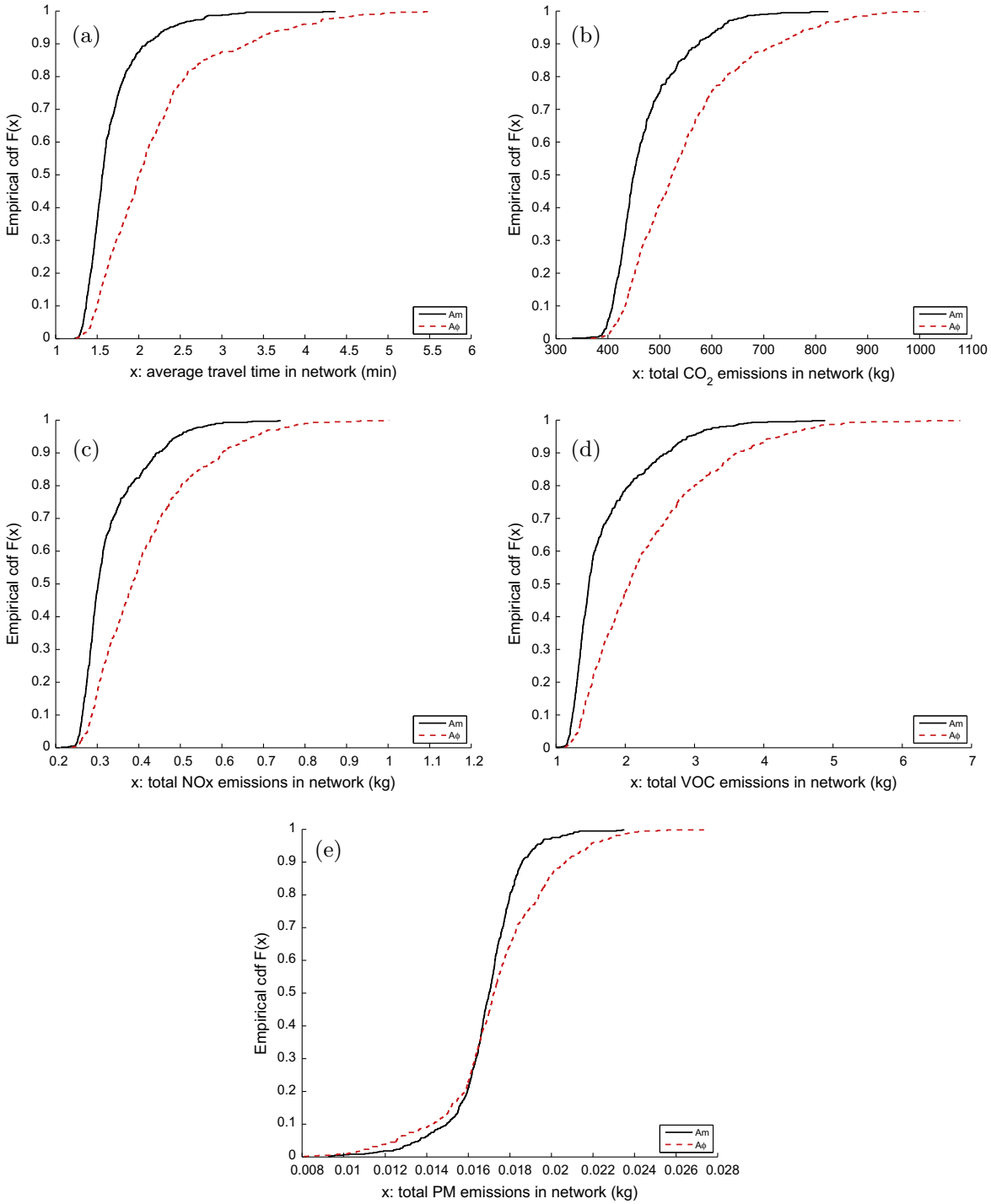

Fig. 4. Summary of the performance of the signal plans derived with Am and $A\phi$ aggregating across all initial points.

by *Am* have significantly better performance than all signal plans proposed by $A\phi$, and than the initial signal and the signal plan proposed by Af_A.

The improved performance of the *Am* plans compared to the $A\phi$ plans shows the added value of embedding the analytical information in the general simulation-based optimization framework. The improved performance of the *Am* plans compared to the Af_A plan shows the added value of using detailed simulated observations to perform optimization. Additional results for a second different initial signal plan are presented in Nanduri et al. (2013). Similar trends and conclusions hold.

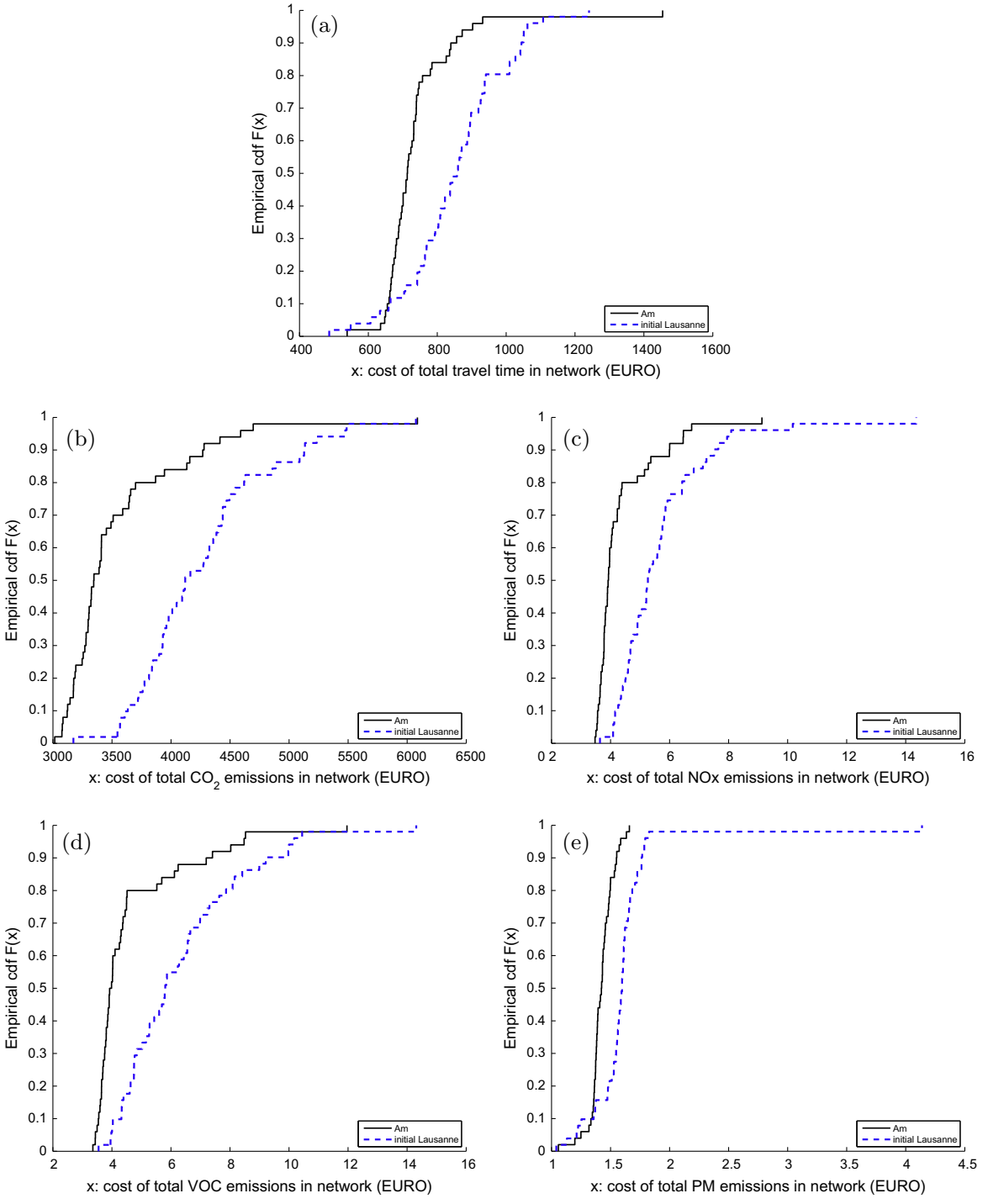

Fig. 5. Monetary evaluation of the best signal plan proposed by *Am* when initialized with an existing signal plan for Lausanne.

Fig. 3 uses the existing signal plan of Lausanne as the initial signal plan. For all five performance metrics, the performance of the signal plan proposed by Af_A is very similar to that of the initial signal plan. Thus, the green curve is barely distinguishable in these plots. Similar conclusions as above hold.

- All plans proposed by *Am* yield similar or better performance compared to the initial plan, and this for all five performance metrics. This is not the case for the plans of $A\phi$ and Af_A. In the case of Af_A, the plan yields, for all metrics, similar performance to the initial plan, there is no metric with improvement. In the case of $A\phi$, one plan does significantly worse than the initial plan for four metrics.
- One plan propose by *Am* outperforms all $A\phi$ plans, as well as all other plans, for all metrics except for PM. For PM, the top 7 plans have very similar performance.
- All plans proposed by *Am* have better or similar performance, for all five metrics, than the plan of Af_A.

We proceed as for the random initial point, and carry out one-sided *t*-tests to evaluate whether the differences observed in Fig. 3 are statistically significant. Table 4 display the corresponding t-statistics. Recall that critical value is -1.68. Statistics below this number indicate that the signal plan proposed by *Am* has significantly better performance. The statistics below this threshold are displayed in bold font in Table 4. This table indicates that all four signal plans proposed by *Am* have significantly better performance than the Lausanne initial plan and than the signal plan proposed by Af_A. They also all outperform signal plan $A\phi(1)$. One of them ($Am(1)$) outperforms $A\phi(4)$. Signal plans $A\phi(2)$ and $A\phi(3)$ are not outperformed by any of the signal plans proposed by *Am*.

Fig. 4 summarizes the information in Figs. 2 and 3. It also includes information from a second initial (randomly generated) point discussed in detail in Nanduri et al. (2013). Each plot of Fig. 4 contains two curves. The solid black curve consists of all the *Am* signal plans displayed in the previously mentioned figures (i.e. each black curve consists of $50 \times 4 \times 3 = 600$ observations of the respective performance measure). Similarly, the dashed red curve consists of all the $A\phi$ signal plans displayed in the previously mentioned figures for that specific performance measure.

Fig. 4 shows that the signal plans proposed by *Am* significantly outperform those proposed by $A\phi$ over four performance metrics namely, average network travel time and total network emissions of CO_2, NO_x and VOC. For the last performance metric (PM emissions), the *Am* plans perform better than the $A\phi$ plans. This shows an added value of using a combination of simulated and analytic information to perform optimizations compared to using just simulated information.

Fig. 5 considers the best signal plan proposed by the method *Am* when initialized with the existing signal plan of Lausanne city. This signal plan corresponds to the signal plan with the lowest objective function estimate. It corresponds to the cdf curve that is the most shifted to the left in Figs. 3(a)–(d). Fig. 5 considers this best plan and demonstrates the monetary savings achieved when this plan is implemented during the one-hour evening peak period from 5 pm to 6 pm on a single day. In order to monetize the reduction in travel time and various pollutant emissions achieved by this plan for the considered network, we use the weights defined in Section 2. As stated in that section, the economic weight parameters for a given pollutant is estimated based on externality costs to human health and other large-scale effects such as global warming. These costs are derived from Table 2 and Table 9 of Mayeres et al. (1996), and listed in Table 5 of Appendix A of this paper.

Fig. 5 contains five plots, each with two curves. The dashed blue curve represents the externality costs for the existing signal configuration of Lausanne city and the solid black curve represents the externality costs when the best *Am* plan is implemented. The externality costs are given in EURO and are calculated for the one-hour evening peak period.

The maximum cost savings are attributable to the reduction in network CO_2 levels followed next by the cost savings from reduction in total network travel time. The reduction in the externality costs of CO_2 emissions in the network ranges (across replications) from 200 to 700 EUROs. It is important to note that these savings are just for the evening peak period on a single day. Travel time savings for the network range (across replications) from 0 to 300 EUROs. Fig. 6 shows the reduction in total externality cost, summed across travel time and all pollutant emissions in the network, achieved by the best *Am* plan over the existing Lausanne plan. This shows that significant cost reductions can be achieved.

Table 5
Problem formulation parameters.

Metric k Unit	w^k [EURO/s] or [EURO/g]	n^k [s] or [g]	C_1^k [g/s]	C_2^k [g/m]	C_3^k [g s/m^2]	C_4^k [g s/m]	C_5^k [g s^3/m^2]	C_6^k [g s^2/m^2]
Travel time T	2.14e−03	109.32						
CO_2	7.72e−03	5.19e+05	5.53e−01	1.61e−01	−2.89e−03	2.66e−01	5.11e−01	1.83e−01
NO_x. If $a_j(t) \geqslant -0.5$ m/s^2	13.8e−03	818.09	6.19e−04	8e−05	−4.03e−06	−4.13e−04	3.80e−04	1.77e−04
NO_x. If $a_j(t) < -0.5$ m/s^2	13.8e−03	818.09	2.17e−04	0	0	0	0	0
VOC. If $a_j(t) \geqslant -0.5$ m/s^2	2.95e−03	1.60e+03	4.47e−03	7.32e−07	−2.87e−08	−3.41e−06	4.94e−06	1.66e−06
VOC. If $a_j(t) < -0.5$ m/s^2	2.95e−03	1.60e+03	2.63e−03	0	0	0	0	0
PM	83.19e−03	106.76	0	1.57e−05	−9.21e−07	0	3.75e−05	1.89e−05

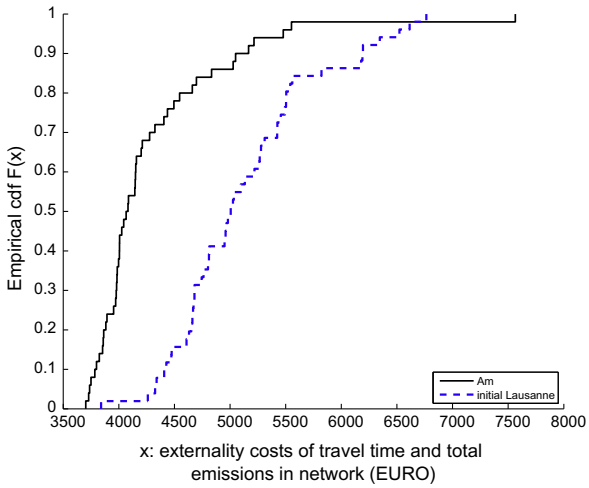

Fig. 6. Monetary evaluation of the best signal plan proposed by *Am* in terms of total externality cost for the network.

Fig. 7 considers the same initial point as Fig. 2. Each plot displays the network of interest. Each link is colored according to the difference in the average (over 50 replications) emissions per vehicle between the best *Am* signal plan and the initial signal plan (i.e., positive values indicate a reduction in emissions achieved by the *Am* signal plan), for the pollutants CO_2, NO_x, VOC and PM, respectively. Links that are colored dark green see a significant reduction in emissions for that specific pollutant, while links colored light green see some reduction. Links colored orange see an increase in pollutant emissions for the *Am* plan compared to the initial plan and links colored red see a significant increase. For each of the four pollutants, we see that overall in the network there is a trend to reduce average emissions at the link-level. Fig. 8 considers the existing signal plan of Lausanne as the initial signal plan. The links display the average difference in emissions between the best plan

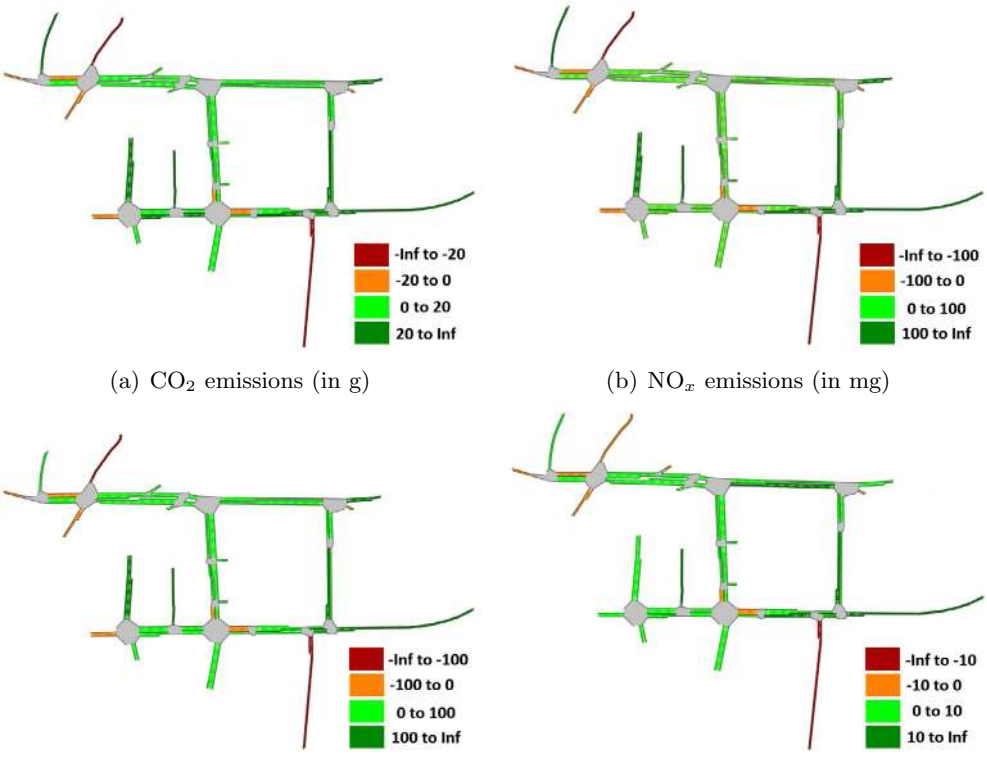

(a) CO_2 emissions (in g) (b) NO_x emissions (in mg)

(c) VOC emissions (in mg) (d) PM emissions (in mg)

Fig. 7. Improvement in average emissions per vehicle per link achieved by the best *Am* plan compared to an initial random signal plan.

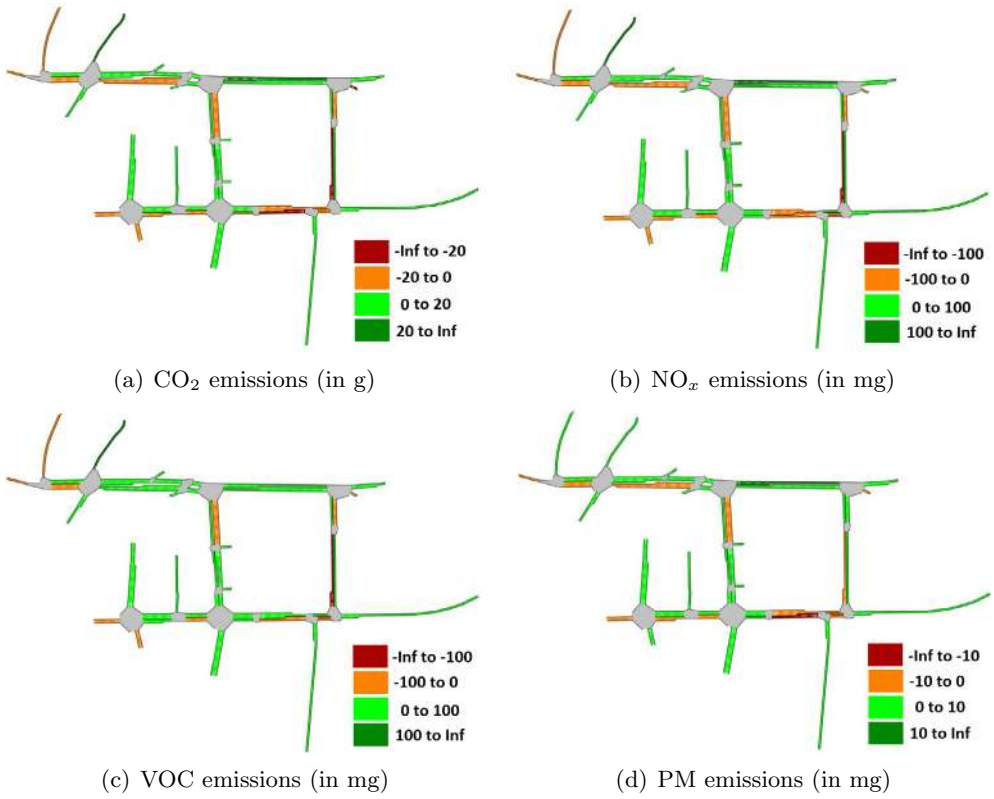

(a) CO_2 emissions (in g) (b) NO_x emissions (in mg)

(c) VOC emissions (in mg) (d) PM emissions (in mg)

Fig. 8. Improvement in average emissions per vehicle per link achieved by the best *Am* plan compared to the Lausanne signal plan.

proposed by *Am* and the Lausanne signal plan. The coloring scheme is the same as for Fig. 7 above. There is, as for the previous figure, an overall link-level improvement, yet it is less marked.

5. Conclusions

This paper proposes a metamodel simulation-based optimization approach to address complex signal control problems that account for environmental metrics. The metamodel is based on a combination of information from a high-resolution microscopic stochastic traffic and emissions simulator with information from a, lower-resolution, macroscopic analytical and differentiable traffic and emissions models.

This paper shows how the combination of low-resolution macroscopic analytical emissions models with high-resolution microscopic simulation emissions models, allows the simulation-based optimization (SO) algorithm to be computationally efficient. More generally, the analysis of this paper highlights the added value of embedding analytical structural information within inefficient SO algorithms in order to efficiently address intricate SO problems.

This paper presents a signal control case study. The signal plans derived by the proposed method typically outperform those derived by methods that resort to only microscopic or only macroscopic information. This shows the superiority of an approach that combines simulated and analytical information, compared to one that is limited to the use of only analytical or only simulated information. Since emissions of pollutants like CO_2, NO_x, VOC and PM depend strongly on individual vehicle attributes and complex local traffic dynamics, they have high variability. Thus, an algorithm which is run under a tight computational budget and uses only simulated information is typically at a disadvantage compared to one that combines suitable analytical and simulated information. This paper also presents the monetary savings which can be achieved with the implementation of a signal plan derived using the proposed framework and indicates that the savings are significant. While the monetary savings are evaluated at the network-level, the empirical analysis also presents the reduction in emissions levels that are achieved at the link-level.

The optimization framework enables the use of high-resolution microscopic traffic and emissions models to go beyond the environmental evaluation of a set of predetermined transportation schemes, and rather to design schemes accounting directly, in the design process, for environmental metrics. Additionally, this work shows the benefits of such an approach both at the local link-level, as well as at a wider network-level. The tight computational budgets used in this paper, show that such complex problems can be addressed in a computationally efficient manner, which is of interest to practitioners.

Since the proposed algorithm is suitable for continuous generally constrained simulation-based optimization problems, it can be used to address a variety of transportation problems. Ongoing work investigates the extension of this method to address dynamic SO problems. For instance, traffic-responsive simulation-based signal control is studied in Chen et al. (2015). The dynamic SO framework of Osorio and Chong (2014) uses a dynamic macroscopic traffic model, and hence is suitable to address optimization problems with time-dependent decision variables (e.g., signal coordination). The ideas in Osorio and Chong (2014) and in Chen et al. (2015) can be combined with the ideas of this paper to design traffic management strategies that account for the spatial–temporal variations of emissions. We are also investigating the added value of combining information from: (i) analytical models, (ii) simulation-based models and (iii) data-driven approaches to address sustainable transportation problems.

Acknowledgments

The authors thank Dr. Emmanuel Bert and Prof. André-Gilles Dumont (LAVOC, EPFL) for providing the Lausanne simulation model. They also thank Prof. Steven Barrett (MIT) for his feedback and guidance in emissions modeling.

Appendix A. Macroscopic traffic model

The physical component of the metamodel is an analytical and differentiable urban traffic model. Each lane of an urban road network is modeled as a set of finite capacity queues. In the following notation the index i refers to a given queue. We refer the reader to Osorio et al. (2010, Chapter 4) and to Osorio and Bierlaire, 2009 for details.

γ_i	external arrival rate;
λ_i	total arrival rate;
μ_i	service rate;
$\tilde{\mu}_i$	unblocking rate;
μ_i^{eff}	effective service rate (accounts for both service andeventual blocking);
ρ_i	traffic intensity;
P_i^f	probability of being blocked at queue i;
s_i	upper bound of thequeuelength;
N_i	totalnumberofvehiclesinqueue i;
$P(N_i = s_i)$	probability of queue i being full, also known as the blocking or spillback probability;
p_{ij}	transition probability from queue$i$to queue j;
$\mathcal{D}_i$	set of downstream queues of queue i;

The queueing network model is formulated as follows.

$$\begin{cases} \lambda_i = \gamma_i + \frac{\sum_j p_{ji}\lambda_j(1-P(N_j=s_j))}{(1-P(N_i=s_i))}, & \text{(a)} \\ \frac{1}{\tilde{\mu}_i} = \sum_{j\in\mathcal{D}_i} \frac{\lambda_j(1-P(N_j=s_j))}{\lambda_i(1-P(N_i=s_i))\mu_j^{\text{eff}}}, & \text{(b)} \\ \frac{1}{\mu_i^{\text{eff}}} = \frac{1}{\mu_i} + P_i^f \frac{1}{\tilde{\mu}_i}, & \text{(c)} \\ P(N_i = s_i) = \frac{1-\rho_i}{1-\rho_i^{s_i+1}}\rho_i^{s_i}, & \text{(d)} \\ P_i^f = \sum_j p_{ij} P(N_j = s_j), & \text{(e)} \\ \rho_i = \frac{\lambda_i}{\mu_i^{\text{eff}}}, & \text{(f)} \end{cases} \tag{26}$$

The exogenous parameters are γ_i, μ_i, p_{ij} and s_i. All other parameters are endogenous. When used to solve a signal control problem (as in this paper), the flow capacity of the signalized lanes become endogenous, which makes the corresponding service rates, μ_i, endogenous.

References

Ahn, K., Rakha, H., 2008. The effects of route choice decisions on vehicle energy consumption and emissions. Transport. Res. Part D 13 (3), 151–167.
Bai, S., Chiu, Y.-C., Niemeier, D., 2007. A comparative analysis of using trip-based versus link-based traffic data for regional mobile source emissions estimation. Atmos. Environ. 41, 7512–7523.
Barceló, J., 2010. Fundamentals of Traffic Simulation. International Series in Operations Research and Management Science, vol. 145. Springer, New York, USA.
Bartin, B., Mudigonda, S., Ozbay, K., 2007. Impact of electronic toll collection on air pollution levels: estimation using microscopic simulation model of large-scale transportation network. Transport. Res. Rec. 2011 (1), 68–77.

Caliper, 2008. TransModeler 4.1 User's Guide.
Cappiello, A., 2002. Modeling Traffic Flow Emissions. Master's Thesis, Massachusetts Institute of Technology. Cambridge, MA, USA.
CARB, 2008. EMFAC 1.0 User's Guide, California Air Quality Research Board.
Chen, X., Osorio, C., Marsico, M., Talas, M., Gao, J.Zhang, S., 2015. Simulation-based adaptive traffic signal control algorithm. In: Transportation Research Board Annual Meeting, Washington DC, USA.
Chiu, Y., Nava, E., Zheng, H., Bustillos, B., 2011. DynusT 3.0 User's Manual.
Dumont, A.G., Bert, E., 2006. Simulation de l'agglomération Lausannoise SIMLO. Technical Report, Laboratoire des voies de circulation, ENAC, Ecole Polytechnique Fédérale de Lausanne.
EPA, 1994. User's Guide to MOBILE5 Mobile Source Emission Factor Model. US Environmental Protection Agency.
EPA, 2003. User's Guide to MOBILE6.1 and MOBILE6.2. US Environmental Protection Agency.
EPA, U., 2010. Motor Vehicle Emission Simulator (MOVES) User Guide. US Environmental Protection Agency.
Kwak, J., Park, B., Lee, J., 2012. Evaluating the impacts of urban corridor traffic signal optimization on vehicle emissions and fuel consumption. Transport. Plan. Technol. 35 (2), 145–160.
Lee, G., You, S.I., Ritchie, S.G., Saphores, J.-D., Sangkapichai, M., Jayakrishnan, R., 2009. Environmental impacts of a major freight corridor. Transport. Res. Rec. 2123 (1), 119–128.
Li, X., Li, G., Pang, S., Yang, X., Tian, J., 2004. Signal timing of intersections using integrated optimization of traffic quality, emissions and fuel consumption. Transport. Res. Part D 9 (5), 401–407.
Lin, J., Chiu, Y., Vallamsundar, S., Bai, S., 2011. Integration of MOVES and dynamic traffic assignment models for fine-grained transportation and air quality analyses. In: IEEE Forum on Integrated and Sustainable Transportation System (FISTS). IEEE, pp. 176–181.
Lin, S., 2011. Efficient Model Predictive Control for Large-scale Urban Traffic Networks. PhD Thesis, Delft University of Technology.
Little, J.D.C., 1961. A proof for the queuing formula: L= λ W. Oper. Res. 9 (3), 383–387.
Little, J.D.C., 2011. Little's law as viewed on its 50th anniversary. Oper. Res. 59 (3), 536–549.
Liu, R., Tate, J., 2000. Microsimulation modeling of intelligent speed adaptation systems. In: European Transport Conference.
Liu, R., 2005. DRACULA 2.3 User Manual, Institute for Transport Studies, University of Leeds, UK. <http://www.its.leeds.ac.uk/software/dracula/tnote2.pdf> (last accessed 17.05.13, 11:20 PM).
Madireddy, M., De Coensel, B., Can, A., Degraeuwe, B., Beusen, B., De Vlieger, I., Botteldooren, D., 2011. Assessment of the impact of speed limit reduction and traffic signal coordination on vehicle emissions using an integrated approach. Transport. Res. Part D 16 (7), 504–508.
Mahmassani, H., Sbayti, H., Zhou, X., 2004. DYNASMART-P Version 1.0 User's Guide.
Mayeres, I., Ochelen, S., Proost, S., 1996. The marginal external costs of urban transport. Transport. Res. Part D 1 (2), 111–130.
Messmer, A., Papageorgiou, M., 1990. Metanet: a macroscopic simulation program for motorway networks. Traffic Eng. Contr. 31, 466–477.
Nanduri, K., 2013. Mitigating Emissions and Energy Consumption for Urban Transportation Networks: Simulation-based Signal Control Strategies. Master's Thesis, Massachusetts Institute of Technology.
Osorio, C., Bierlaire, M., 2009. An analytic finite capacity queueing network model capturing the propagation of congestion and blocking. Eur. J. Oper. Res. 196 (3), 996–1007.
Osorio, C., Bierlaire, M., 2013. A simulation-based optimization framework for urban transportation problems. Oper. Res. 61 (6), 1333–1345.
Osorio, C., Chong, L., 2014b. A simulation-based optimization algorithm for dynamic traffic control problems. In: Transportation Science and Logistics (TSL) Workshop.
Osorio, C., Chong, L., 2014a. A computationally efficient simulation-based optimization algorithm for large-scale urban transportation. Transport. Sci. (forthcoming). <http://web.mit.edu/osorioc/www/papers/osoChoLgeScaleSO.pdf>.
Osorio, C., Nanduri, K., 2014. Energy-efficient urban traffic management: a microscopic simulation-based approach, Transport. Sci. (forthcoming). <http://web.mit.edu/osorioc/www/papers/osoNanEnergySO.pdf>.
Osorio, C., 2010. Mitigating Network Congestion: Analytical Models, Optimization Methods and Their Applications. PhD Thesis, Ecole Polytechnique Fédérale de Lausanne.
Osorio, C., Chen, X., Marsico, M., Talas, M., Gao, J., Zhang, S., 2014. Reducing gridlock probabilities via simulation-based signal control. In: Proceedings of the International Symposium of Transport Simulation (ISTS).
Osorio, C., Flötteröd, G., Zhang, C., 2014. A metamodel simulation-based optimization approach for the efficient calibration of stochastic traffic simulators. In: Proceedings of the International Symposium of Transport Simulation (ISTS).
Panis, L., Broekx, S., Liu, R., 2006. Modeling instantaneous traffic emission and the influence of traffic speed limits. Sci. Total Environ. 371, 270–285.
Park, B., Yun, I., Ahn, K., 2009. Stochastic optimization for sustainable traffic signal control. Int. J. Sustain. Transport. 3 (4), 263–284.
PTV, 2008. VISSIM 4.30 User's Manual. Planung Transport Verkehr AG, Karlsruhe, Germany.
Quadstone, 2009. PARAMICS v5.0 Modeller Reference Manual.
QUARTET, 1992. Assessment of Current Tools for Environment Assessment in QUARTET, Drive II Project V2018.
Rakha, H., Van Aerde, M., Ahn, K., Trani, A., 2000. Requirements for evaluating traffic signal control impacts on energy and emissions based on instantaneous speed and acceleration measurements. In: Transportation Research Board Annual Meeting, Washington DC, USA.
Rakha, H., Ahn, K., Trani, A., 2003. Comparison of MOBILE5a, MOBILE6, VT-MICRO and CMEM models for estimating hot-stabilized light-duty vehicle emissions. Can. J. Civ. Eng. 30 (6), 1010–1021.
Rakha, H., Ahn, K., Trani, A., 2004. Development of VT-Micro model for estimating hot stabilized light duty vehicle and truck emissions. Transport. Res. Part D 9 (1), 49–74.
Scora, G., Barth, M., 2006. Comprehensive Modal Emission Model (CMEM) Version 3.01 User's Guide. University of California, Riverside.
Smit, R., Smokers, R., Rabe, E., 2007. A new modeling approach for road traffic emissions. Transport. Res. Part D 12, 414–422.
Stafford, R., 2006. The Theory Behind the 'randfixedsum' Function. <http://www.mathworks.com/matlabcentral/fileexchange/9700>.
Stevanovic, J., Stevanovic, A., Martin, P.T., Bauer, T., 2008. Stochastic optimization of traffic control and transit priority settings in VISSIM. Transport. Res. Part C 16 (3), 332–349.
Stevanovic, A., Stevanovic, J., Zhang, K., Batterman, S., 2009. Optimizing traffic control to reduce fuel consumption and vehicular emissions. Integrated approach with VISSIM, CMEM, and VISGAOST. Transport. Res. Rec. 2128, 105–113.
Tijms, H.C., 2003. A First Course in Stochastic Models. Wiley, Chichester, West Sussex, England.
TSS, 2011. AIMSUN 6.1 Microsimulator Users Manual. Transport Simulation Systems.
Van Aerde, M., 1999. INTEGRATION Release 2.20 User's Guide. Van Aerde and Assoicates.
VSS, 1992. Norme Suisse SN 640837 Installations de feux de circulation; temps transitoires et temps minimaux. Union des professionnels suisses de la route, VSS, Zurich.
Williams, L., Yu, L., 2001. A Conceptual Examination of the Impact of Traffic Control Strategies on Vehicle Emission and Fuel Consumption. Technical Report SWUTC/01/467203, Texas Southern University.
Xie, Y., Chowdhury, M., Bhavsar, P., Zhou, Y., 2011. An integrated tool for modeling the impact of alternative fueled vehicles on traffic emissions: a case study of Greenville, South Carolina. In: Transportation Research Board Annual Meeting, Washington DC, USA.
Zegeye, S., Schutter, B., Hellendoorn, H., Breunesse, E., 2010. Model-based traffic control for balanced reduction of fuel consumption, emissions and travel time. In: Proceedings of the 12th IFAC Symposium on Transportation Systems, Redondo Beach, CA, USA.
Zhang, L., Yin, Y., Chen, S., 2013. Robust signal timing optimization with environmental concerns. Transport. Res. Part C 29, 55–71.